Photochemical & Photobiological Sciences

PAPER

Cite this: *Photochem. Photobiol. Sci.*, 2017, **16**, 201

Parietin: an efficient photo-screening pigment *in vivo* with good photosensitizing and photodynamic antibacterial effects *in vitro*†

Laura R. Comini,[a] F. Eduardo Morán Vieyra,[b] Ricardo A. Mignone,[b] Paulina L. Páez,[c] M. Laura Mugas,[a] Brenda S. Konigheim,[d] José L. Cabrera,[a] Susana C. Núñez Montoya*[a] and Claudio D. Borsarelli*[b]

Received 8th September 2016,
Accepted 27th November 2016

DOI: 10.1039/c6pp00334f

rsc.li/pps

The photophysical, photoinduced pro-oxidant and antibacterial properties *in vitro* of the natural occurring parietin (PTN; 1,8-dihydroxy-3-methoxy-6-methyl-9,10-anthraquinone) were evaluated. PTN was extracted from the lichen identified as *Teloschistes flavicans* (Sw.) Norm. (Telochistaceae). Results indicate that in chloroform solution, PTN presents spectroscopic features corresponding to an excited-state intramolecular proton-transfer (ESIPT) state with partial keto–enol tautomerization. In argon-saturated solutions, the singlet excited state is poorly fluorescent (Φ_F = 0.03), decaying by efficient intersystem crossing to an excited triplet state ^{3}PTN*, as detected by laser-flash photolysis experiments. In the presence of triplet molecular oxygen, the ^{3}PTN* was fully quenched producing singlet molecular oxygen ($^1O_2$) with a quantum yield of 0.69. In addition, in buffer solutions, PTN has the ability to also generate a superoxide radical anion ($O_2^{\bullet-}$) in a human leukocyte model and its production was enhanced under UVA-Vis irradiation. Finally, the *in vitro* antibacterial capability of PTN in the dark and under UVA-Vis illumination was compared in microbial cultures of both Gram positive and negative bacteria. As a result, PTN showed promising photo-induced antibacterial activity through the efficient photosensitized generation of both $^1O_2$ and $O_2^{\bullet-}$ species. Thus, we have demonstrated that PTN, an efficient photo-screening pigment in lichens, is also a good photosensitizer in solution with promising applications in antibacterial photodynamic therapy.

1. Introduction

Parietin or physcion (PTN, Scheme 1) is an anthraquinone pigment found as a secondary metabolite in lichens, *e.g. Xanthoria parietina.*[1] This pigment is located as tiny extracellular crystals at the top layer of the upper cortex of lichens and it is responsible for their strong orange-brownish coloration playing a photo-protective role against solar radiation.[1,2] In particular, it has been found that the light screening effect of PTN is functionally more important in the blue-light than the UVB region.[2] Moreover, antibacterial and antifungal activity of PTN has been reported,[3,4] and recently its ability to produce apoptosis in several types of human cancer cells has been demonstrated.[5,6]

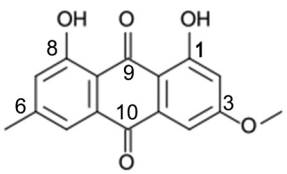

Scheme 1 Structure of parietin (1,8-dihydroxy-3-methoxy-6-methyl-9,10-anthraquinone).

Our current research interest is based on the characterization of natural active compounds present in Argentinean flora, focusing on antibacterial, antiviral and anticancer activities of anthraquinone derivatives.[7,8] In the last few years, we have also characterized the photodynamic activity *in vitro* of the natural anthraquinones, whose effects are mainly driven

[a]*IMBIV, CONICET and Facultad de Ciencias Químicas, Universidad Nacional Córdoba, Haya de la Torre y Medina Allende, X5000HUA Córdoba, Argentina. E-mail: sununez@fcq.unc.edu.ar*
[b]*Instituto de Bionanotecnología del NOA (INBIONATEC), Universidad Nacional de Santiago del Estero – CONICET, RN9, Km 1125, G4206XCP Santiago del Estero, Argentina. E-mail: cdborsarelli@gmail.com*
[c]*Dto. Farmacia, Facultad de Ciencias Químicas, Universidad Nacional de Córdoba, Unidad de Tecnología Farmacéutica (UNITEFA) – CONICET, Haya de la Torre y Medina Allende, X5000HUA Córdoba, Argentina*
[d]*Instituto de Virología "Dr. J.M. Vanella", Facultad de Ciencias Médicas, Universidad Nacional de Córdoba, Ciudad Universitaria, X5000HUA Córdoba, Argentina*
† Electronic supplementary information (ESI) available: Spectroscopic and chromatographic information of parietin purification. See DOI: 10.1039/c6pp00334f

by the generation of reactive oxygen species (ROS), *i.e.* superoxide radical anion ($O_2^{\bullet -}$), hydroxyl radical ($HO^{\bullet}$) and singlet molecular oxygen ($^1O_2$).[9,10]

Hence, following our research interest in searching for natural pigments with potential photosensitizing properties, in this work, we have extracted and purified PTN from a lichen identified as *Teloschistes flavicans* (Sw.) Norm. (Telochistaceae) with the aim of evaluating its spectroscopic, photophysical, photosensitizing properties and capability of generation of reactive oxygen species (ROS) in air-saturated solutions, in addition to whether it has antibacterial effects mediated by photosensitization.

2. Experimental

2.1. Materials

All organic solvents were of HPLC grade and purchased from Sintorgan SRL (Buenos Aires, Argentina). To eliminate residual water, chloroform ($CHCl_3$) was doubly distilled using quicklime as a drying agent. Organic and inorganic compounds were obtained from Sigma (St Louis, MO, USA) and used as received. The following reagents were used: Eagle's minimum essential medium (EMEM, Gibco, USA), Fetal calf serum (FCS, Natocor, Argentina), L-glutamine (GlutaMAX, Gibco, France), gentamicin (EMEVE, Argentina), dimethyl sulfoxide (DMSO, Tetrahedron, Argentina), Neutral Red (NR, Gibco, USA), and phosphate buffer saline (PBS). *Teloschistes flavicans* was collected in January 2012, in Tucuman province, Argentina (GPS coordinates: 26° 51′ 25.0″ South latitude; 65° 40′ 33.9″ West longitude). It was identified by Drs C. Estrabou and J. M. Rodriguez (CERNAR, Facultad de Ciencias Físicas y Naturales, Universidad Nacional de Córdoba, Argentina). A voucher specimen was deposited at the Museo Botánico de Córdoba (U.N.C.) as CORDC 3647.

2.2. Parietin extraction and purification

Dried and fragmented lichen (100 g) was exhaustive macerated with ethanol (EtOH) overnight. Isolation of PTN from the dried EtOH extract was performed by combining Column Chromatography (CC) with preparative Thin Layer Chromatography (p-TLC). A portion of the EtOH extract was subjected to Sephadex LH-20 CC (Sigma-Aldrich, MO, USA), eluted with a stepwise gradient of $CHCl_3$–AcOEt, AcOEt–acetone, acetone–EtOH (10 : 0; 8 : 2; 1 : 1; 2 : 8; 0 : 10, respectively). The eluents were analyzed by TLC (silica gel 60G, Macherey-Nagel, Duren, Germany) with *n*-ButOH–acetic acid–water (BAW, 4 : 1 : 5) as a mobile phase, and revealed under UV light with NH_4OH fumes. Fractions with similar TLC patterns were combined to give two major fractions (A–B). PTN was purified from fraction A by p-TLC and using the same mobile phase mentioned above (BAW, 4 : 1 : 5). Finally, PTN was identified by their spectroscopic and spectrometric data (UV-Vis, MS, ^{1}H and ^{13}C NMR, including 2D NMR experiments, see the ESI†), which were coincident with those previously reported in the literature.[11–13] The final PTN purity was 96.2 ± 0.6%, as determined by HPLC analysis (ESI†). Varian Pro Star chromatography apparatus (model 210, Agilent, CA, USA), equipped with an UV-Vis detector and a Microsorb-MV column 100-5 C-18 (250 × 4.6 mm i.d.), was used at 25 °C. The mobile phase was a gradient elution of formic acid 0.16 M dissolved in ultrapure water (solvent A) and MeOH–formic acid 0.16 M (solvent B), whose composition was changed from 65 to 0% of solvent A in 66 min, with a variable flow from 1 at 0.7 mL min^{-1}. The detector was set at 265 nm. The sample was dissolved in MeOH (HPLC grade, Sintorgan, Buenos Aires, Argentina), filtered through cellulose (Merck Millipore, Sao Paulo, Brazil) and manually injected (20 μL). Data analysis was performed using the Varian software (Star Chromatography Workstation 6.41).

2.3. Spectroscopic methods

UV-Vis absorption spectra were recorded with an Agilent 8453 diode array spectrophotometer (Agilent, Palo Alto, CA, USA). Fluorescence emission and excitation spectra were recorded with a Hitachi F-2500 spectrofluorimeter (Kyoto, Japan), using excitation and emission slits of 2.5 nm bandwidth. Fluorescence quantum yield (Φ_F) of PTN was determined in $CHCl_3$ by excitation at 420 nm of several samples with $A_{420} < 0.1$; and compared with those of disodium fluorescein in 0.1 N NaOH aqueous solution (Φ_F = 0.95) as a fluorescence standard with eqn (1),[14]

$$\Phi_{F(S)} = \Phi_{F(R)} \times \frac{F_S A_R {n_S}^2}{F_R A_S {n_R}^2} \quad (1)$$

where F, A, and n are fluorescence integrated areas, the absorbance value at the excitation wavelength and the refractive index of the solvent used for the PTN sample (S) and fluorescein reference (R).

Fluorescence decays of PTN in $CHCl_3$ solution were obtained with a time-correlated single photon counting (TSCPC) fluorimeter Tempro-01 (Horiba, Glasgow, UK), using 1 MHz pulsed LED emitting at 390 nm (fwhm 15 nm). Fluorescence detection was performed using a −30 °C cooled photomultiplier tube detector with <10 dark counts (TBX-07C, Horiba), placed in the output of an f/4 emission monochromator with an emission slit of 12 nm. A diluted Ludox scatter solution was used to register the instrumental response at the excitation wavelength and also to verify that no excitation scattered light was acquired at the emission wavelength. The fluorescence intensity was fitted with the fluorescence decay analysis software DAS6® (Horiba) by deconvolution of the pulse function, using the multi-exponential model function eqn (2), where n is the number of single exponential decays, τ_i and α_i are the decay time and the fluorescence intensity amplitude at t = 0 of each decay, respectively.

$$I(t) = \sum_{i=1}^{n} \alpha_i \exp(-t/\tau_i) \quad (2)$$

The average lifetime (τ_{av}) was calculated using the fractional fluorescence contribution of each decay time f_i; eqn (3).[14]

$$\tau_{av} = \sum_{i=1}^{n} f_i \tau_i; \quad \text{with } f_i = \frac{\alpha_i \tau_i}{\sum_{i=1}^{n} \alpha_i \tau_i} \tag{3}$$

The decay associated spectrum (DAS), which is the emission spectrum associated with the *i*-th decay component, $I_i(\lambda)$, was calculated by the product of the steady-state emission spectrum $I_{ss}(\lambda)$ with the fractional contribution of each decay time at each emission wavelength, $f_i(\lambda)$, using $\alpha_i(\lambda)$ and τ_i from the global exponential fitting analysis routine, eqn (4).

$$I_i(\lambda) = f_i(\lambda) I_{ss}(\lambda) = \frac{\alpha_i(\lambda)\tau_i}{\sum_i \alpha_i(\lambda)\tau_i} I_{ss}(\lambda) \tag{4}$$

The transient absorption spectrum of PTN was registered with a home-made laser-flash photolysis system using as an excitation source a Nd:YAG pulsed laser operating with the third harmonic at 355 nm (Minilite II, Continuum Inc., Santa Clara, CA, USA, 3 mJ per pulse, 7 ns fwhm, 2 Hz). The laser beam was directed at a right angle to the analyzing beam from a 175 W Xenon arc lamp (Luzchem, Canada) synchronized with a controlled shutter (Uniblitz; VMM-T1 Vincent Associates, Rochester, NY, USA). The detection system comprises a f/4 Czerny Turner monochromator with 1200 lines per mm (PTI-101, Photon Technology International, Lawrenceville, NJ, USA) with an attached R3788 photomultiplier (Hamamatsu Photonics, Japan). Transient signals were acquired with a 300 MHz digital oscilloscope (Tektronix TDS3032B, Tektronix Inc., Wilsonville, OR, USA), and up to 30 single shot signals were averaged. Triplet decays were analyzed using OriginPro 8.5® software (OriginLab Corp. Northampton, MA, USA).

Time-resolved phosphorescence detection of singlet oxygen ($^1O_2$) was done using a home-made system,[15] composed of a Peltier cooled Ge photodiode (Judson J16TE2-66G, Teledyne Judson Technology, Montgomeryville, PA, USA) placed at a right angle to the excitation of a Nd:YAG pulsed laser at 355 nm. Spurious light was filtered with a 1270 nm band pass filter (Spectrogon BP-1260, Spectrogon Inc., Parsippany, NJ, USA). In all cases, the transient signals were fed to the Tektronix TDS3032B digital oscilloscope. The quantum yield (Φ_Δ) of $^1O_2$ production of PTN in $CHCl_3$ was determined by actinometry using phenalenone (PN) in $CHCl_3$ solutions as a reference compound with $\Phi_\Delta = 0.95 \pm 0.05$.[16] Typically, about 20–30 transient signals were averaged into the digital oscilloscope, and afterwards fed into a PC and processed with the OriginPro 8.5® software.

2.4. Superoxide radical anion ($O_2^{\bullet-}$) quantification

The production of $O_2^{\bullet-}$ was detected and quantified by an indirect bioassay that measures the reduction of Nitroblue Tetrazolium (NBT) to Nitroblue Diformazan (NBF), by action of $O_2^{\bullet-}$ generated inside human leukocytes in the presence of an oxidizer, such as anthraquinones.[9,10] Human leukocytes, from voluntary and healthy donors, were used within four hours after their extraction. Trypan blue dye exclusion was employed to test the viability of the leukocyte suspension. This suspension was subjected to a combined Dextran/Ficoll-Hypaque sedimentation procedure to separate neutrophils from monocytes, following the methodology described previously.[7,8] Afterwards, neutrophils were washed twice with Hanks' Balanced Salt Solution (HBSS) and suspended in the same buffer. PTN was dissolved in HBSS solution using a small amount of DMSO (<1 μL) as a co-solvent. In the NBT assay, 0.1 mL of neutrophils solution (10^6 mL^{-1}) in HBSS at pH 7 was incubated with 0.1 mL of PTN solution (between 9 μM and 350 μM) and 0.5 mL of NBT (0.1% P/V) at 37 °C for 30 min. The samples were centrifuged at 1500*g* for 10 min after stopping the reaction with the addition of 0.1 M HCl (0.1 mL). The supernatant was separated and the sediment was extracted with 1 mL of DMSO. This procedure was performed in the dark and under irradiated conditions in order to evaluate the PTN capability to increase $O_2^{\bullet-}$ generation relative to the case in the absence of PTN (control). The irradiation source (described in section 2.7) was placed inside a black box at 50 cm above a thermostatic bath containing the samples. In all cases (samples and controls both in the dark and under irradiation conditions), the absorbance of intracellular NBF was measured at 575 nm. All experiments were performed in duplicate. The *t*-test was used to assess the degree of statistical difference between the increase in percentage of $O_2^{\bullet-}$ evaluated in the dark and under irradiation. Differences between means were considered significant at $p < 0.05$.

2.5. *In vitro* antibacterial activity of parietin

The bactericidal effect of PTN against two Gram positive bacteria (*Staphylococcus aureus* ATCC 29213 and *Staphylococcus epidermidis* ATCC 12228) and two Gram negative bacteria (*Escherichia coli* ATCC 25922 and *Pseudomonas aeruginosa* ATCC 27853) was evaluated by the micro-dilution method according to Clinical & Laboratory Standards Institute (CLSI).[17] Minimum Inhibitory Concentration (MIC) and Minimum Bactericidal Concentration (MBC) were determined using the Mueller Hinton broth (MH, Britania SRL, Buenos Aires, Argentina). An overnight culture of each microorganism was diluted to achieve a cell density in the range from $1 \times 10^{(6\pm1)}$ colony-forming units per milliliter (CFU mL^{-1}), and incubated for 10 min at 37 °C. PTN, dissolved in phosphate buffer saline (PBS) and DMSO as a co-solvent (<1%), was serially diluted (1 : 2) from 250 to 0.125 μg mL^{-1} in a 96-well plate ($n = 2$ for each concentration tested). Then, the bacterial suspension (100 μL) was added into each well to obtain a total volume of 200 μL. Bacterial growth was observed after 18 h of incubation. The lowest concentration of PTN that prevented bacterial growth was considered the MIC. Viable bacterial counts were obtained for samples without visible bacterial growth by plating on MH agar, followed by aerobic incubation at 37 °C for 18 h. PTN concentration that produces the death of 99.9% of initial inoculum was considered the MBC. This assay was simultaneously repeated under actinic irradiation at intervals of 10 min with a total irradiation time of 2 h, using the irradiation system placed inside a black box at 30 cm above the multi-well plate containing the samples. Controls of

irradiation and in the dark (without PTN) were carried out under the same conditions.

2.6. *In vitro* cytotoxicity assay

The cytotoxicity of PTN was tested on the Vero cell line 76 ATCC CRL-587, following the methodology described by Konigheim *et al.*[18] A confluent monolayer of cells [approximately (1.0 ± 0.6) × 10^5 cells per well; 24 h incubation] was treated with 15 consecutive dilutions of PTN in triplicate, within a range of 1 to 500 μg mL^{-1}. Cell controls (CC) were included (n = 3). The assay was simultaneously performed in the dark and under irradiation conditions for 15 min with the described light system, placed 9 cm above the microplates. After incubation (48 at 37 °C), the cellular viability (CV) was measured by means of the neutral red (NR) uptake by live cells. The absorbance of the NR extracted was measured at 540 nm on a microplate reader (BioTek ELx800). The percentage of CV was calculated by comparison with cell controls (100% viability). From the plot of CV% *vs.* PTN concentration, the concentration of the compound that reduces the viable cells was determined by regression ($R^2 > 0.9$).

2.7. Irradiation source for *in vitro* assays

As PTN pigment in solution absorbs blue-light,[11,19] we have chosen a Phillips actinic lamp (TL 20 W/52, 380–480 nm, 0.65 mW cm^{-2}) with a maximum at 420 nm, usually used in phototherapy treatment of human hyperbilirubinemia (http://www.philips.com/phototherapy) as an excitation source for superoxide radical anion generation, antibacterial activity and cytotoxicity under illuminated conditions (see above).

3. Results and discussion

3.1. Spectroscopic and singlet-excited state properties

Fig. 1 shows the UV-Vis absorption spectrum of 24 μM PTN in $CHCl_3$. The intense absorption bands at UV-B ($\lambda_{ab}^{max} \approx 290$ nm) and in the blue-light portion (λ_{ab}^{max} = 438 nm; $\lambda_{ab}^{shoulder}$ = 455 nm) have also been reported for PTN in acetone[1] and EtOH[19,20] solutions. For anthraquinones, a low intense $^1(n,\pi)^*$ transition is expected to occur at ≈414 nm.[21–24] However, due to the presence of electron donor –OH groups at positions 1 and 8, a red-shifted intense $^1(\pi,\pi)^*$ transition rather than a $^1(n,\pi)^*$ transition can be expected as dominant for the lowest absorption band ($S_0 \rightarrow S_1$) of PTN.[21,22]

The fluorescence emission spectrum of PTN observed by excitation at 420 nm in $CHCl_3$ solution showed a broad band between 450–750 nm with a maximum at 505 nm and shoulders at 530 nm and 575 nm (Fig. 1). PTN dissolved in EtOH also shows similar spectral features with a maximum at 509 nm and a shoulder at 530 nm.[20] The excitation fluorescence spectrum registered at an emission wavelength of 500 nm was almost coincident with the UV-Vis absorption spectrum, despite the different spectral resolution and instrumental responses between both types of measurements, *e.g.* ±1 nm and ±2.5 nm for UV-Vis and fluorescence spectra,

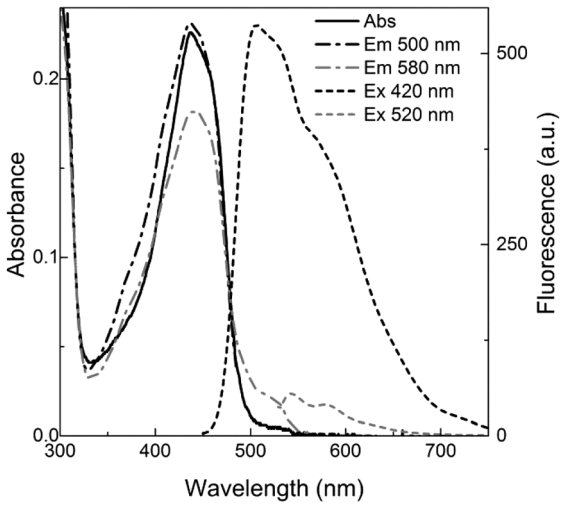

Fig. 1 UV-Vis absorption spectrum (solid black line), fluorescence excitation spectra with λ_{em} = 500 nm (dash–dot black line) and with λ_{em} = 580 nm (dash–dot gray line); and fluorescence emission spectra with λ_{ex} = 420 nm (dashed black line) and with λ_{ex} = 520 nm (dashed grey line) of 24 μM parietin in air-saturated $CHCl_3$ solutions.

respectively. However, the excitation spectra monitored with emission at 580 nm showed an additional red-shifted band around 520 nm. In effect, a tiny absorption band at the same region can be observed in the absorption spectrum of PTN. Excitation of this absorption band at 520 nm displayed weak emission with spectral maxima at 540 and 577 nm. Thus, these results suggest that PTN emits from at least two different excited states. From the wavelength crossing between the normalized absorption and emission spectra, the lowest excited singlet state energy was estimated, *i.e.* E_S = 60.0 ± 0.2 kcal mol^{-1}. This value agrees with that for 1,8-dihydroxyanthraquinone (1,8-DHAQ), which can be considered as the parent compound of PTN, with E_S = 61.3 kcal mol^{-1} in acetonitrile[21] and E_S = 60.3 kcal mol^{-1} in *n*-octane at 10 K.[24]

On the other hand, despite the external heavy-atom quenching effect of the chlorine atoms of the $CHCl_3$ solvent, PTN still emits with a fluorescence quantum yield of Φ_F = 0.03 ± 0.01, both in argon- and air-saturated solutions. This value is closer to $\Phi_F \approx 0.02$–0.05 reported for anthraquinone derivatives with electron-donor substituents as –OH groups, which induce dominant $^1(\pi,\pi)^*$ transitions.[23,25] The relatively large Stokes-shift of ≈70 nm for the intense absorption band indicates a large change of dipolar moment of the lowest singlet excited state of PTN, *e.g.* ^{1}PTN*. As the emission maximum of PTN in $CHCl_3$ (ε_r = 4.81) was almost the same as in EtOH (ε_r = 24.5), the observed Stokes-shift cannot be linked to general solvent polarity effects.[14]

Fig. 2a confirms that the fluorescence decays of PTN are dependent on the monitoring emission wavelength. In all cases, satisfactory fittings (*i.e.* lower χ^2 together with uniform residual and autocorrelation function plots oscillating around zero) were only obtained by using a three-exponential decay function for the deconvolution procedure, eqn (2). The

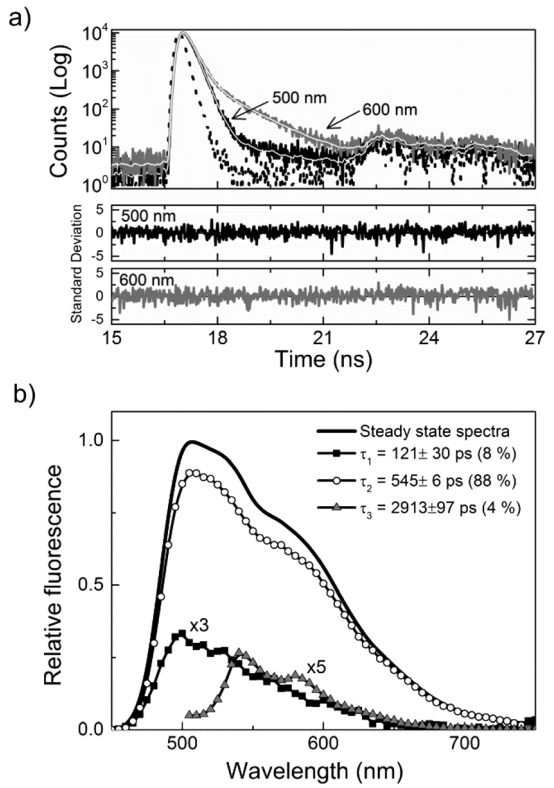

Fig. 2 (a) Fluorescence emission decays (black lines) of 24 μM parietin in air-saturated $CHCl_3$ observed at 500 nm and 600 nm, together with the instrumental response signal (gray line) and the respective residual plots after fitting by deconvolution analysis using a three-exponential function. Excitation with Nanoled® at 390 nm (15 fwhm) operating at 1 MHz. (b) Decay associated spectra (DAS) of ^{1}PTN* obtained after global analysis of the fluorescence decay of PTN as a function of wavelength. Note that minor contributions were amplified by factors of 3 and 5, respectively, for better visualization.

recovered fractional fluorescence contribution (f_i) and respective lifetimes (τ_i) at 500 nm indicated that the fluorescence decay was practically dominated by a component of 530 ps (91.3%), with minor contribution of a faster decay of 110 ps (7.9%), yielding an average lifetime τ_{av} = 533 ps as calculated with eqn (3). This ultra-short average lifetime value was closer to that observed for 1,8-DHAQ in several organic solvents.[21,23] However, a different lifetime distribution at 600 nm was observed, with a long-lived contribution resulting in a longer average lifetime of 837 ps. In any case, the ultra-short average lifetime of ^{1}PTN* (<1 ns) explains the similar low Φ_F value in both argon- and air-saturated $CHCl_3$ solutions.

A more complete description of the dynamic behavior of ^{1}PTN* as a function of the emission wavelength can be obtained by means of the decay associated spectra (DAS), as shown in Fig. 2b. The global fitting analysis of the fluorescence decays between 450 and 750 nm with steps of 5 nm, indicates that the main decay component of 545 ps (88%) is associated with spectral emission similar to the steady-state spectrum obtained with excitation at 420 nm, *i.e.* a maximum at 505 nm and a shoulder at 575 nm. The shorter lifetime of 112 ps contributing with 8% displays a blue-shifted emission maximum at 498 nm. Finally, the minor contribution (4%) with a lifetime of 2.9 ns shows similar emission spectra as the steady-state spectrum observed with excitation at 520 nm.

The above steady-state and dynamic fluorescence behavior of PTN can be explained in terms of an excited-state intramolecular proton-transfer (ESIPT) mechanism operating for anthraquinones with hydroxyl substituents in adjacent positions to the keto groups, Scheme 1.[23,24] In the excited state, the phenolic –OH becomes more acidic than in the ground state, while the carbonyl oxygen of the keto group is more basic. Thus, for 1-OH anthraquinone derivatives, the ESIPT process produces a large molecular rearrangement from 9,10-keto to 1,10-keto tautomeric forms (Scheme 2), lowering the singlet excited state energy and producing red-shifted emission by relaxation to the ground state. It has been reported that this type of molecule possess potential functions along the proton transfer coordinate with double-minimum energy surfaces in both ground and excited states.[23,24] In the case of PTN, the blue-shifted emission (λ_{em}^{max} = 498 nm) can be associated with the decay of normal (N*) form of the excited singlet state of PTN, while the dual emission at the red-edge (λ_{em}^{max} = 505 and $\lambda_{em}^{sh} \approx$ 575 nm) is dominated by the decay of the tautomeric (T*) excited state species. As PTN also contains different substituents, *e.g.* C_3–OCH_3 and C_6–CH_3, it is also an asymmetric molecule and therefore a multi-exponential decay behavior can be expected for the red-shifting emission of the T* states formed by proton-transfer of the adjacent C_1–OH or C_8–OH to the C_9=O, respectively. Nevertheless, considering that the purity degree of PTN was checked as ≈96% and the high responsiveness of the TCSPC technique, the lowest fluorescence contribution with a longer associated lifetime and red-shifted emission could be also assigned to an impurity effect.

3.2. Triplet excited state and singlet oxygen $^1O_2$ production

The triplet excited state of PTN (^{3}PTN*) in Ar-saturated $CHCl_3$ solution was detected by laser flash photolysis experiments. Fig. 3 shows the transient absorption spectra of PTN obtained after pulsed laser excitation at 355 nm. Multiple transient absorption bands centered at 340, 480 and 650 nm were observed, with similar features to the transient spectrum of 1,8-DHAQ in isopropyl alcohol.[26] All these transient bands

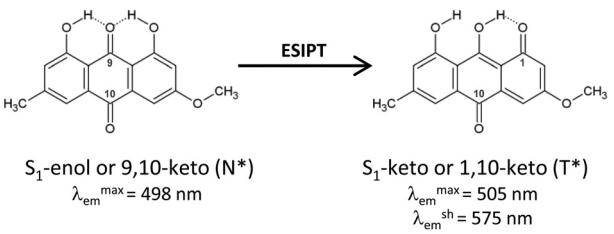

Scheme 2 Molecular structures of the enol (left) and keto (right) tautomeric species of PTN produced by an excited-state intramolecular proton-transfer (ESIPT) mechanism.

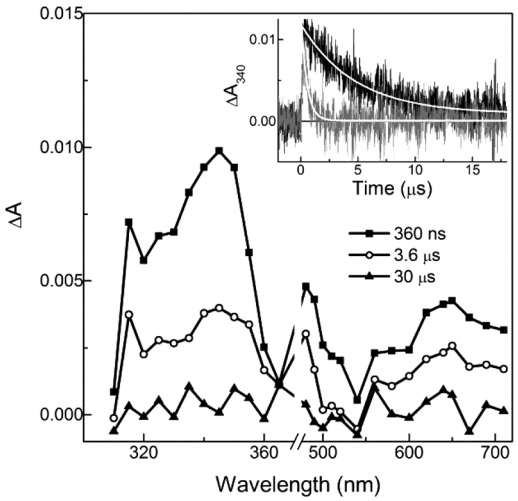

Fig. 3 Transient absorption spectrum of 80 μM parietin in argon-saturated $CHCl_3$ solution observed at different times after the laser pulse at 355 nm. Inset: Transient decay monitored at 340 nm in Ar-saturated (black line) and in O_2 (5%)/N_2-saturated $CHCl_3$ solutions.

decayed with similar lifetime, and hence the ^{3}PTN* lifetime monitored at 340 nm in argon-saturated solution was τ_T = 5.0 ± 0.2 μs. However, in air-saturated solutions (21% dissolved oxygen, *i.e.* $[O_2]$ = 2.4 mM) no transient signal was detected, suggesting that the ^{3}PTN* lifetime was shortened below the experimental time resolution of our LFP set-up, *e.g.* <100 ns. In order to estimate the bimolecular quenching rate constant of ^{3}PTN* by $^3O_2$, *i.e.* ^3k_q, the transient decay at 340 nm was also monitored in $CHCl_3$ solution saturated with a N_2/O_2 mixture containing 5% of $^3O_2$ (≈0.12 mM). In such a case, the ^{3}PTN* decayed with a shorter lifetime of 510 ± 40 ns (inset of Fig. 3). Thus, $^3k_q \approx 1.4 \times 10^{10}$ M^{-1} s^{-1} was estimated by using eqn (5), where $\tau_{T,0}$ and τ_T are the triplet lifetimes in the absence and presence of 5% of $^3O_2$, respectively.

$$^3k_q = (\tau_T{}^{-1} - \tau_{T,0}{}^{-1})/[O_2]_{5\%} \quad (5)$$

Hence, in air-saturated solutions almost full quenching of ^{3}PTN by $^3O_2$ can be expected since the quenching efficiency $^3\eta_q$ (= $^3k_q[O_2]/(\tau_{T,0}{}^{-1} + {}^3k_q[O_2]_{21\%})) \approx 1$.

Gollnick *et al.*[21] demonstrated that both triplet quantum yield Φ_T and singlet oxygen quantum yield (Φ_Δ) of hydroxyanthraquinones dissolved in acetonitrile were dependent on the energy level of the S_1 $^1(\pi,\pi^*)$ state compared with that of the corresponding T_2 $^3(n,\pi^*)$ state, producing a very fast intersystem crossing followed by internal conversion processes to populate the lowest T_1 $^3(\pi,\pi^*)$ state. In the case of anthraquinone derivatives with E_S above or below E_{T_2} (up to ±1.5 kcal mol^{-1}), efficient intersystem crossing was produced with $\Phi_T \geq 0.70$ and $\Phi_\Delta \geq 0.65$, as it was in the case of 1,8-DHAQ.[21]

As mentioned above, the singlet state energy E_S of PTN in $CHCl_3$ was closer to that of 1,8-DHAQ in acetonitrile,[21] hence a small energy gap between the S_1 $^1(\pi,\pi^*)$ and T_2 $^3(n,\pi^*)$ states can also be assumed for PTN. In such a case, efficient generation of $^1O_2$ can be expected after excitation of PTN in aerated solutions. Indeed, the inset of Fig. 4 shows the transient phosphorescence signal of $^1O_2$ in air-saturated $CHCl_3$ at room temperature generated after 355 nm pulsed laser excitation of 80 μM PTN. The growth time of the phosphorescence signal of $^1O_2$, which is equivalent to the triplet lifetime of PTN in the presence of air, is within the time resolution of our Ge-detector (<300 ns) as expected for a diffusion-controlled quenching process of ^{3}PTN* by $^3O_2$ in air-saturated organic solvents through an energy-transfer (type II) mechanism,[27] eqn (6).

$$^3\text{PTN}^* + {}^3O_2 \xrightarrow{\eta_q \approx 1} \text{PTN} + {}^1O_2 \quad (6)$$

In such a case, the decay portion of the transient phosphorescence intensity $I_{(t)}$ of $^1O_2$ can be fitted with a single exponential function eqn (7), where I_0 is the initial phosphorescence intensity and τ_Δ is the lifetime of $^1O_2$.

$$I_{(t)} = I_0 \times \exp(-t/\tau_\Delta) \quad (7)$$

A τ_Δ = 215 (±4) μs was obtained, as it can be expected for the decay of $^1O_2$ in $CHCl_3$ solutions,[28] and it was the same as that observed using phenalenone (PN) as a sensitizer (data not shown). Therefore, it can be concluded that PTN does not quench $^1O_2$ under the concentration condition used in the experiment, *e.g.* 80 μM.

The quantum yield of formation of $^1O_2$ (Φ_Δ) by sensitization of PTN was determined by extrapolation of the initial intensity (I_0) of the $^1O_2$ signal by the first-order fitting of the phosphorescence decay, due to the proportionality of I_0 with Φ_Δ, eqn (8).

$$I_0 = \kappa k_p \Phi_\Delta (1-10^{-A_{355}}) E_l^{355} = k \Phi_\Delta E_{ab} \quad (8)$$

In this equation κ is the proportionality instrumental constant, k_p is the solvent-specific radiative decay rate constant

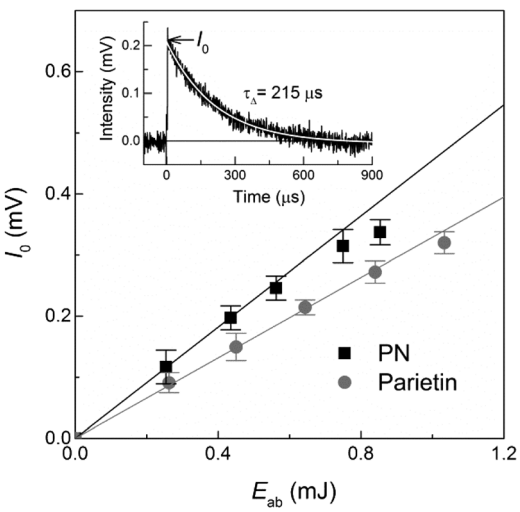

Fig. 4 Dependence of the initial intensity of the $^1O_2$ phosphorescence signal I_0 as a function of the absorbed energy E_{ab} of excitation laser at 355 nm (eqn (8)) of 80 μM parietin in air-saturated $CHCl_3$ solution. Inset: Averaged transient phosphorescence signal of $^1O_2$ observed with E_{ab} = 0.64 mJ. White line represents the exponential data fitting with eqn (7).

for $^1O_2$, E_l^{355} is the incident laser energy and A_{355} is the solution absorbance at the laser excitation wavelength. Thus, from the comparison of the linear plots of I_0 *vs.* absorbed laser energy E_{ab} for PTN and reference PN[16] in the same solvent (Fig. 4), $\Phi_\Delta = 0.69 \pm 0.02$ was calculated for PTN. This result confirms that $\Phi_T \geq 0.69$, as mentioned above. Furthermore, the same Φ_Δ value was reported for 1,8-DHAQ in acetonitrile solutions,[21] confirming that the photophysical properties of PTN are closer to those for the parent compound 1,8-DHAQ. To the best of our knowledge, this is the first report of Φ_Δ for PTN, indicating that it behaves as an efficient photosensitizer in solution, such as the case of other relevant hydroxyanthraquinone derivatives, *e.g.* 2-hydroxy-anthraquinone ($\Phi_\Delta = 0.68$), 1,2,5,8-tetrahydroxy-anthraquinone (quinalizarin, $\Phi_\Delta = 0.27$) and 3-methyl-1,6,8-trihydroxyanthraquinone (emodin, $\Phi_\Delta = 0.82$).[29]

3.3. Superoxide radical anion $O_2^{\bullet-}$ production

The production of $O_2^{\bullet-}$ was evaluated by means of the conventional NBT assay.[10] The polymorphonuclear neutrophils (PMNs), the most abundant circulating blood leukocytes,[30] were selected because they are good $O_2^{\bullet-}$ generators in response to a given stimulus. Indeed, in these cells the $O_2^{\bullet-}$ production is a fundamental factor in host defense mechanisms against microorganisms.[31] Fig. 5 shows the relative amount of $O_2^{\bullet-}$ produced when neutrophils were treated with increasing concentrations of PTN in the dark and under actinic radiation (380–480 nm) for 30 min relative to the respective controls (neutrophils without PTN in the dark and under irradiation conditions). The controls represent the basal production of $O_2^{\bullet-}$ by the neutrophils, and it was the same ($p > 0.01$) for both dark and irradiated conditions (dashed line). The $O_2^{\bullet-}$ generation in the presence of PTN followed a Gaussian-like shape as a function of the anthraquinone concentration on the log scale, with a maximum response around 35 μM PTN (Fig. 5). In the dark, the addition of PTN induced up to a seven-times increase of $O_2^{\bullet-}$ relative to the basal production, an expected effect because of the exacerbated NADPH-oxidase activity in the oxidative respiratory burst in response to exogenous stimuli, eqn (9).[31,32]

$$2O_2 + NADPH \rightarrow 2O_2^{\bullet-} + NADP^+ + H^+ \quad (9)$$

Irradiation of neutrophils with PTN up to 35 μM, increases significantly the intracellular amount of $O_2^{\bullet-}$, obtaining almost twice of radical species that at the same concentration of PTN in the dark. This behavior is the result of an electron-transfer (type I) mechanism by photosensitization of PTN by the reaction of ^{3}PTN* with a sacrificial reducing substrate R, eqn (10) and (11).[9,10]

$$^3PTN^* + R \rightarrow PTN^{\bullet-} + R^{\bullet+} \quad (10)$$

$$PTN^{\bullet-} + {}^3O_2 \rightarrow PTN + O_2^{\bullet-} \quad (11)$$

Similar results have been found for other plant anthraquinones, which were also proposed as efficient type I photosensitizers, since the production of $O_2^{\bullet-}$ was also dependent on both anthraquinone concentration and irradiation.[9,10] However, under both dark and irradiated conditions at larger PTN concentration than 35 μM, the production of $O_2^{\bullet-}$ was strongly reduced, obtaining relative values closer or below those for the basal generation. This type of behavior has been also reported for other compounds in neutrophils, such as chloramphenicol, which produced the optimum stimuli of intracellular $O_2^{\bullet-}$ at 4 μg mL^{-1}, but above this concentration the total antioxidant was exceeded by the enhanced oxidative stress that turned out noxious for cells leading to a decrease in this ROS.[33] Thus, at higher xenobiotic concentration levels, the overproduction of $O_2^{\bullet-}$ resulted in harmful oxidative stress to neutrophils leading to a decrease of the cell metabolism. In addition to this effect, as the PTN intracellular concentration increases self-aggregation effects could also play a role, since the formation of PTN aggregates in neutral and acidic solutions even at concentration lower than 10 μM has been observed.[34] The lower $O_2^{\bullet-}$ production observed under irradiated conditions than in the dark at PTN concentrations above 35 μM (Fig. 5) confirms the intracellular self-aggregation of PTN, since anthraquinone aggregation abates their photophysical and photobiological activities by quenching both singlet and triplet excited states.[35]

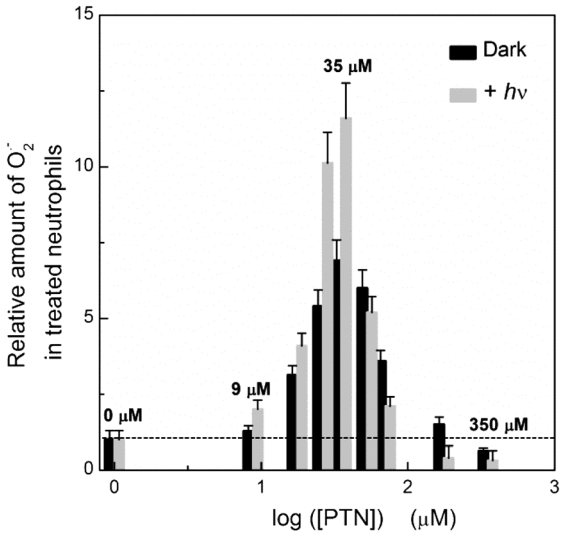

Fig. 5 Relative superoxide anion radical $O_2^{\bullet-}$ generation in neutrophils produced at different concentrations of PTN, assessed by NBT reduction assay in the dark and with illumination under actinic radiation (380–480 nm) with respect to respective controls without PTN.

3.4. Dark and photo-induced antibacterial activity

Routine susceptibility tests, including the determination of Minimum Inhibitory Concentration (MIC) and Minimum Bactericidal Concentration (MBC), are quantitative parameters of bacteriostatic and bactericidal actions.[36] Typically, plant compounds with MIC values in the range of 100–1000 μg mL^{-1} are classified as "moderately antimicrobial", while plant compounds with MIC values equal or lower than 100 μg mL^{-1} are considered good antimicrobial agents.[36]

Table 1 Dark and photoinduced Minimum Inhibitory Concentration (MIC) and Minimum Bactericidal Concentration (MBC) elicited by parietin

	MIC (μg mL^{-1})		MBC (μg mL^{-1})		
Bacterial spp.	Dark	+$h\nu$	Dark	+$h\nu$	MIC/MBC + $h\nu$
S. aureus ATCC 29213	>250	16	n.a.	>64	0.25
S. epidermidis ATCC 12228	>250	<0.13	n.a.	>0.5	0.25
E. coli ATCC 25922	>250	250	n.a.	250	1.00
P. aeruginosa ATCC 27853	>250	0.5	n.a.	0.5	1.00

n.a.: Not applicable. SD = 5%.

In the dark, PTN did not exhibit any antibacterial effect up to 250 μg mL^{-1} (≈880 μM) against all bacterial strains tested (Table 1), *e.g.* two Gram positive bacteria (*Staphylococcus aureus* and *Staphylococcus epidermidis*) and two Gram negative bacteria (*Escherichia coli* and *Pseudomonas aeruginosa*). These results are in line with those reported by Manojlovic *et al.*,[4] who stated that PTN showed good antibacterial activity against *Bacillus subtilis and Pseudomonas fluorescens* (MIC = 80 μg mL^{-1}), but showed moderate activity against *S. aureus* (MIC = 320 μg mL^{-1}) and no activity against *E. coli* up to 320 μg mL^{-1}.

Conversely, under irradiation the inhibitory effect of PTN on *S. epidermidis* and *S. aureus* was strongly increased, with MIC values <0.13 μg mL^{-1} (≈0.5 μM) and 16 μg mL^{-1} (56 μM), respectively (Table 1). These values are similar to those employed for known synthetic antibiotics like ciprofloxacin and gentamicin, *e.g.* 0.25 ≤ MIC (μg mL^{-1}) ≤ 32.[37–40] Thus, the irradiation enhances the antibacterial effect of PTN, turning it into a good photodynamic antibacterial agent. This phenomenon is similar to that observed for other natural photosensitizing anthraquinones such as rubiadin and soranjidiol, both isolated from the vegetal species *H. pustulata*, which exhibit significant increases in their antibacterial activity under irradiation at 10 μg mL^{-1} (bactericidal activity) compared to dark conditions (bacteriostatic activity).[8] More interesting, PTN showed bacteriostatic activity against both Gram positive (MIC/MBC = 0.25) and bactericidal activity on Gram negative (MIC/MBC = 1) bacteria, unlike the majority of compounds from lichens, which generally inhibit mainly the growth of Gram positive bacteria.[41]

Under irradiation, PTN also showed a marked antimicrobial effect in strains with natural ability to form biofilms, as *S. epidermidis* and *P. aeruginosa* (Table 1). The latter microorganism is responsible for severe infections and often shows a high resistance to conventional antibiotics.[6] In this context, a comparison with other recognized photosensitizers suggests that PTN could be a suitable photodynamic agent against this resilient bacterium. For instance, toluidine blue O, an effective antibacterial photosensitizer of various bacterial species showed, under irradiation, bactericidal activity against four strains of *P. aeruginosa*, at concentrations between 7.5 and 10 μM.[42] Banfi *et al.*[43] found that for a series of photosensitizing porphyrins, only the derivative (5,15-di(*N*-(4-methoxybenzyl)-4-pyridyl)-10,20-di(4-pyridyl) porphyrin dichloride) showed a photodynamic bactericide effect against *P. aeruginosa* at low concentration of 7.3 μM, whereas for the rest the same effect was observed at concentration between 15–35 μM. Interestingly, hypericin, a natural photosensitizer considered for the new generation of photodynamic therapy drugs, did not show photodynamic antibacterial activity against *P. aeruginosa* at concentrations between 0.2 and 20 μM.[44] Hence, the efficient photodynamic antimicrobial effect of PTN against *P. aeruginosa*, with MIC = MBC = 0.5 μg mL^{-1} (1.7 μM) (Table 1), makes this compound combined with UVA-blue light a suitable treatment for this resilient microorganism.

Most importantly, our results about cytotoxicity of PTN in Vero cells showed that cellular viability at a concentration of 100 μg mL^{-1} was ≈80% and 60% in the dark and under irradiation, respectively. Nevertheless, the active concentrations (bacteriostatic/bactericidal) of PTN against *S. aureus, S. epidermidis* and *P. aeruginosa* under irradiation conditions (Table 1) are well below those concentrations.

Altogether, the results of Table 1 point out PTN as an efficient photodynamic antibacterial agent for bacteria killing, probably mediated by the combination of $^1O_2$ and $O_2^{\bullet-}$ formed upon irradiation. The microorganisms during metabolic processes also produce ROS; however, when the rate of generation of free radicals is higher than the rate of their detoxification, bacteria suffer "oxidative stress".[45] Thus, for example, the ROS are a powerful oxidant of biological macromolecules and they can interact with several cytoplasmic and nuclear components by reaction with lipids, proteins and DNA,[46] which results in an inactivation that leads to the death of different microorganisms. In this framework, it is worth mentioning that natural anthraquinone photosensitizers, have demonstrated a good antibacterial effect in combination with light, by setting a close relationship with the ROS production (particularly, $^1O_2$),[8] and allowing their application in protocols of Antimicrobial Photodynamic Therapy (APTD) as a potential technique to inactivate numerous bacteria without the development of new resistant strains.[47,48]

4. Conclusion

The present results demonstrate that PTN, a pigment found in some lichens as tiny crystals acting as photo-screens against UVB and blue light,[1,19] in dilute $CHCl_3$ solution showed spectroscopic properties typical of hydroxy-anthraquinone

derivatives with excited-state intramolecular proton-transfer (ESIPT) producing keto–enol tautomerization. In turn, the triplet excited state ^{3}PTN*, as detected by transient absorption spectroscopy, was populated with similar efficiency to the parent 1,8-dihydroxianthraquinone compound, *e.g.* Φ_T = 0.7. In air-saturated solutions, the ^{3}PTN* was fully quenched by $^3O_2$ to produce $^1O_2$ (Φ_Δ = 0.69 ± 0.02). In aqueous suspension of neutrophil cells, PTN was also able to generate $O_2^{\bullet-}$ with double efficiency under irradiated conditions than in the dark. Thus, by UVA-Vis illumination of air-saturated PTN solutions both $^1O_2$ and $O_2^{\bullet-}$ are generated. These results reveal a completely opposite function of this molecule *in vivo*, where PTN acts as a UV-blue light photo-screen in lichens, since is forming tiny crystals.[1,2] In fact, PTN showed promising photo-induced killing activity against both Gram positive and negative bacteria, *e.g. S. aureus*, *S. epidermidis*, and *P. aeruginosa* at concentrations that do not affect normal mammalian cells appreciably.

Altogether, these results indicate that PTN behaves as a good type I and type II photosensitizer by UVA-blue light irradiation with promising application in Antimicrobial Photodynamic Therapy (APTD) for the treatment of local infections.[48,49] Further studies are currently being performed to reveal the detailed mechanism of cell death induction.

Acknowledgements

C. D. B. thanks the financial support of Argentinean funding agencies CONICET (PIP-2012-0374) and FONCyT (PICT-2012-2666 and PICTO-UNSE-2012-0013), and the Alexander von Humboldt Foundation of Germany for equipment subsidy. L. R. C., S. C. N. M. and J. L. C. thank the financial support of CONICET (PIP-2013-4316), SeCyT-UNC-2014-203 and FONCYT (PICT-2010-1576). The authors are thankful to Drs C. Estrabou and J. M. Rodríguez (CERNAR, Facultad Ciencias Físicas y Naturales, Universidad Nacional de Córdoba) for identification of the vegetal species, and Dr G. Bonetto (Laboratorio de RMN, INFIQC, CONICET and UNC) for performing the NMR experiments.

References

1 K. Solhaug and Y. Gauslaa, *Oecologia*, 1996, **108**, 412–418.
2 Y. Gauslaa and E. M. Ustvedt, *Photochem. Photobiol. Sci.*, 2003, **2**, 424–432.
3 S. K. Agarwal, S. S. Singh, S. Verma and S. Kumar, *J. Ethnopharmacol.*, 2000, **72**, 43–46.
4 N. T. Manojlovic, S. Solujic and S. Sukdolak, *Lichenologist*, 2002, **34**, 83–85.
5 M. Bačkorová, R. Jendželovský, M. Kello, M. Bačkor, J. Mikeš and P. Fedoročko, *Toxicol. in Vitro*, 2012, **26**, 462–468.
6 A. Basile, D. Rigano, S. Loppi, A. Di Santi, A. Nebbioso, S. Sorbo, B. Conte, L. Paoli, F. De Ruberto, A. M. Molinari, L. Altucci and P. Bontempo, *Int. J. Mol. Sci.*, 2015, **16**, 7861–7875.
7 L. R. Comini, I. M. Fernandez, N. B. R. Vittar, S. C. Núñez Montoya, J. L. Cabrera and V. A. Rivarola, *Phytomedicine*, 2011, **18**, 1093–1095.
8 L. R. Comini, S. C. Núñez Montoya, P. L. Páez, G. A. Argüello, I. Albesa and J. L. Cabrera, *J. Photochem. Photobiol., B*, 2011, **102**, 108–114.
9 L. R. Comini, S. C. Núñez Montoya, M. Sarmiento, J. L. Cabrera and G. A. Argüello, *J. Photochem. Photobiol., A*, 2007, **188**, 185–191.
10 S. C. Núñez Montoya, L. R. Comini, M. Sarmiento, C. Becerra, I. Albesa, G. A. Argüello and J. L. Cabrera, *J. Photochem. Photobiol., B*, 2005, **78**, 77–83.
11 J. W. Fairbairn and F. J. El-Muhtadi, *Phytochemistry*, 1972, **11**, 263–268.
12 P. Canaviri, K.-E. Bergquist and J. Vila, *Rev. Boliv. Quim.*, 2006, **23**, 9–12.
13 T.-S. Wu, T.-T. Jong, H.-J. Tien, C.-S. Kuoh, H. Furukawa and K.-H. Lee, *Phytochemistry*, 1987, **26**, 1623–1625.
14 J. R. Lakowicz, *Principles of fluorescence spectroscopy*, Springer Science+Business Media, LLC, Singapore, 2006.
15 C. D. Borsarelli, M. Mischne, A. La Venia and F. E. Moran Vieyra, *Photochem. Photobiol.*, 2007, **83**, 1313–1318.
16 R. Schmidt, C. Tanielian, R. Dunsbach and C. Wolff, *J. Photochem. Photobiol., A*, 1994, **79**, 11–17.
17 R. A. Boulos, N. Y. T. Man, N. A. Lengkeek, K. A. Hammer, N. F. Foster, N. A. Stemberger, B. W. Skelton, P. Y. Wong, B. Martinac, T. V. Riley, A. J. McKinley and S. G. Stewart, *Chem. – Eur. J.*, 2013, **19**, 17980–17988.
18 B. S. Konigheim, L. R. Comini, S. Grasso, J. J. Aguilar, J. Marioni, M. S. Contigiani and S. C. N. Montoya, *Lat. Am. J. Pharm.*, 2012, **31**, 51–56.
19 K. A. Solhaug, Y. Gauslaa, L. Nybakken and W. Bilger, *New Phytol.*, 2003, **158**, 91–100.
20 O. Castro Mandujano, A. Pastor de Abram and I. E. Collantes Díaz, *Rev. Soc. Quim. Peru*, 2011, **77**, 152–161.
21 K. Gollnick, S. Held, D. O. Mártire and S. E. Braslavsky, *J. Photochem. Photobiol., A*, 1992, **69**, 155–165.
22 A. Navas Diaz, *J. Photochem. Photobiol., A*, 1990, **53**, 141–167.
23 D. K. Palit, H. Pal, T. Mukherjee and J. P. Mittal, *J. Chem. Soc., Faraday Trans.*, 1990, **86**, 3861–3869.
24 G. Smulevich, P. Foggi, A. Feis and M. P. Marzocchi, *J. Chem. Phys.*, 1987, **87**, 5664–5669.
25 N. S. Allen, G. Pullen, M. Shah, M. Edge, D. Holdsworth, I. Weddell, R. Swart and F. Catalina, *J. Photochem. Photobiol., A*, 1995, **91**, 73–79.
26 H. Pal, D. K. Palit, T. Mukherjee and J. P. Mittal, *J. Photochem. Photobiol., A*, 1991, **62**, 183–193.
27 F. Wilkinson, *Pure Appl. Chem.*, 1997, **69**, 851–856.
28 F. Wilkinson, W. P. Helman and A. B. Ross, *J. Phys. Chem. Ref. Data*, 1995, **24**, 663–677.
29 R. W. Redmond and J. N. Gamlin, *Photochem. Photobiol.*, 1999, **70**, 391–475.
30 E. Di Carlo, G. Forni, P. Lollini, M. P. Colombo, A. Modesti and P. Musiani, *Blood*, 2001, **97**, 339–345.

31 H. Sim Choi, J. Woo Kim, Y. N. Cha and C. Kim, *J. Immunoassay Immunochem.*, 2006, **27**, 31–44.
32 E. E. Ritchey, J. D. Wallin and S. V. Shah, *Kidney Int.*, 1981, **19**, 349–358.
33 P. L. Páez, M. C. Becerra and I. Albesa, *Basic Clin. Pharmacol. Toxicol.*, 2008, **103**, 349–353.
34 E. Lopez-Tobar, V. Verebova, L. Blascakova, D. Jancura, G. Fabriciova and S. Sanchez-Cortes, *Spectrochim. Acta, Part A*, 2016, **159**, 134–140.
35 K. Tobias, K. Barbara and P. Kristjan, *Curr. Med. Chem.*, 2006, **13**, 2189–2204.
36 G. Tegos, F. R. Stermitz, O. Lomovskaya and K. Lewis, *Antimicrob. Agents Chemother.*, 2002, **46**, 3133–3141.
37 M. C. Becerra, M. Sarmiento, P. L. Páez, G. Argüello and I. Albesa, *J. Photochem. Photobiol., B*, 2004, **76**, 13–18.
38 I. L. D. Galera, M. G. Paraje and P. L. Páez, *J. Biol. Nat.*, 2016, **5**, 122–130.
39 M. C. Becerra, P. L. Páez, L. E. Laróvere and I. Albesa, *Mol. Cell. Biochem.*, 2006, **285**, 29–34.
40 B. Hellmark, M. Unemo, Å. Nilsdotter-Augustinsson and B. Söderquist, *Clin. Microbiol. Infect.*, 2009, **15**, 238–244.
41 *Lichen Biol*, ed. I. Nash and H. Thomas, Cambridge University Press, 2008.
42 S. P. Tseng, L. J. Teng, C. T. Chen, T. H. Lo, W. C. Hung, H. J. Chen, P. R. Hsueh and J. C. Tsai, *Lasers Surg. Med.*, 2009, **41**, 391–397.
43 S. Banfi, E. Caruso, L. Buccafurni, V. Battini, S. Zazzaron, P. Barbieri and V. Orlandi, *J. Photochem. Photobiol., B*, 2006, **85**, 28–38.
44 N. Kashef, Y. S. Borghei and G. E. Djavid, *Photodiagn. Photodyn. Ther.*, 2013, **10**, 150–155.
45 V. I. Lushchak, *Biochemistry*, 2001, **66**, 476–489.
46 A. K. D. Cavalcante, G. R. Martinez, P. Di Mascio, C. F. M. Menck and L. F. Agnez-Lima, *DNA Repair*, 2002, **1**, 1051–1056.
47 C. M. N. Yow, H. M. Tang, E. S. M. Chu and Z. Huang, *Photochem. Photobiol.*, 2012, **88**, 626–632.
48 K. D. Winckler, *J. Photochem. Photobiol., B*, 2007, **86**, 43–44.
49 C. Pellieux, A. Dewilde, C. Pierlot and J.-M. Aubry, in *Methods Enzymol.*, Academic Press, 2000, 319, 197–207.